Laser Photolysis of Chromium(III) Porphyrins with Axial Pyridines in Dichloromethane and Toluene Solutions. Novel Effects of a Hydrogen Bond in the Ligand Exchange Reaction

Masahiko Inamo,* Hideyuki Nakaba, and Kiyohiko Nakajima

Department of Chemistry, Aichi University of Education, Kariya, Aichi 448-8542, Japan

Mikio Hoshino

The Institute of Physical and Chemical Research, Wako, Saitama 351-0198, Japan

Received February 24, 2000

Laser photolysis studies were carried out for (chloro)(pyridine)(5,10,15,20-tetraphenylporphyrinato)chromium(III), [Cr(TPP)(Cl)(Py)], in both dichloromethane and toluene containing water. The five-coordinate [Cr(TPP)(Cl)] produced by the photoinduced dissociation of pyridine from [Cr(TPP)(Cl)(Py)] initially reacts with H_2O to give [Cr(TPP)(Cl)(H_2O)], which eventually exchanges the axial H_2O with Py to regenerate [Cr(TPP)(Cl)(Py)]. The rate for the ligand exchange of [Cr(TPP)(Cl)(H_2O)] with exogenous Py is found to exhibit a bell-shaped pyridine-concentration dependence. Kinetic studies revealed that at a high Py concentration, the exogenous Py probably makes a hydrogen bond with the axial H_2O of [Cr(TPP)(Cl)(H_2O)] to yield [Cr(TPP)(Cl)(HO−H···Py)] as a dead-end complex. A similar structure of the Cr−TPP complex having 2-methylpyridine molecules bound to the coordinated H_2O ligand by a hydrogen bond was determined by X-ray structure analysis. The exchange reaction of the axial HO−H···Py in [Cr(TPP)(Cl)(HO−H···Py)] by Py follows the dissociative mechanism: the first step is the dissociation of Py from [Cr(TPP)(Cl)(HO−H···Py)], and the second step is the dissociation of H_2O. The five-coordinate [Cr(TPP)(Cl)] thus produced reacts with Py to regenerate [Cr(TPP)(Cl)(Py)]. The direct ligand exchange reaction of the axial HO−H···Py in [Cr(TPP)(Cl)(HO−H···Py)] with exogenous Py does not occur. Probably, the hydrogen bond, HO−H···Py, increases the basicity of H_2O, and thus, the bond energy between Cr and O in [Cr(TPP)(Cl)(HO−H···Py)] becomes much stronger than that in [Cr(TPP)(Cl)(H_2O)]. The mechanism of the ligand substitution reaction of the chromium(III) porphyrins has been examined in detail on the basis of the laser photolysis studies of [Cr(TPP)(Cl)(L)] (L = pyridine, 3-cyanopyridine, and H_2O).

Introduction

Although chromium(III) porphyrins are not naturally occurring substrates in biological systems, their chemical and photochemical properties have been extensively studied since the ability of the various metalloporphyrins to characterize hemoproteins was recognized. Among the various aspects of their chemical features, interactions between metalloporphyrins and axial ligands have been focused on in relation to the oxygen binding ability of hemoproteins. It is commonly recognized that the substitution reactions of the axial ligands of metalloporphyrins proceed much faster than those of other metal complexes. These effects were well documented for the metalloporphyrins with substitution-inert metal ions such as chromium(III),[1,2] which undergo the ligand exchange reaction based on the dissociative mechanism. The dissociative mechanism of the ligand exchange reactions of metalloporphyrins assumes the coordinately unsaturated intermediate as a reactive species. Some of the six-coordinate metalloporphyrins efficiently undergo photochemical dissociation of the axial ligand to yield the coordinately unsaturated intermediate.[3] Thus, the laser photolysis technique has provided useful information on the ligand exchange reaction of the metalloporphyrins via coordinately unsaturated intermediates.

Studies on the photochemistry of the chromium(III) porphyrins have revealed that the nature of the excited states of the complex can be interpreted in terms of weak coupling of the π excited states of the porphyrin ligand and the d electrons of the central chromium(III) ion, giving singquartet ($^4S_1$), tripdoublet ($^2T_1$), tripquartet ($^4T_1$), and tripsextet ($^6T_1$) excited states.[4] A laser photolysis study of the chromium(III) porphyrins [Cr(TPP)(Cl)(L)] (L is an axial ligand) has revealed that photoinduced physical and chemical processes depend on both the nature of the bond between chromium and the axial ligand L as well as the complex environment.[5−10] The mechanism of the photoreaction of chromium porphyrins has been discussed on the basis of the laser photolysis studies, which revealed that the photoelimination of the axial ligand L occurs via two reaction paths, i.e., the path through the $^4S_1$ and $^6T_1$ excited states, and that the yield of the photoelimination largely depends on the donor ability of the axial ligand L.[10] It was found that the coordinately

(1) Fleischer, E. B.; Krishnamurthy, M. *J. Am. Chem. Soc*. **1971**, *93*, 3784.
(2) O'Brien, P.; Sweigart, D. A. *Inorg. Chem*. **1982**, *21*, 2094.
(3) Sima, J. *Struct. Bonding* **1995**, *84*, 135.
(4) Gouterman, M.; Hanson, L. K.; Khalil, G.-E.; Leenstra, W. R.; Buchler, J. W. *J. Chem. Phys.* **1975**, *62*, 2343.
(5) Yamaji, M.; Hama, Y.; Hoshino, M. *Chem. Phys. Lett.* **1990**, *165*, 309.
(6) Yamaji, M. *Inorg. Chem.* **1991**, *30*, 2949.
(7) Inamo, M.; Hoshino, M.; Nakajima, K.; Aizawa, S.; Funahashi, S. *Bull. Chem. Soc. Jpn.* **1995**, *68*, 2293.
(8) Hoshino, M.; Tezuka, N.; Inamo, M. *J. Phys. Chem.* **1996**, *100*, 627.
(9) Hoshino, M.; Nagamori, T.; Seki, H.; Chihara, T.; Tase, T.; Wakatsuki, Y.; Inamo, M. *J. Phys. Chem. A* **1998**, *102*, 1297.
(10) Inamo, M.; Hoshino, M. *Photochem. Photobiol.* **1999**, *70*, 596.

10.1021/ic0002059 CCC: $19.00
Published on Web 09/06/2000

unsaturated intermediate generated by the photoinduced axial ligand dissociation reacts with a water molecule present in the toluene solution to give [Cr(TPP)(Cl)(H_2O)] as an intermediate during the photoreaction of [Cr(TPP)(Cl)(3-CNPy)] (3-CNPy = 3-cyanopyridine).[7]

In the present work, the photoreaction of [Cr(TPP)(Cl)(Py)] in the dichloromethane and toluene solutions was studied using a laser photolysis technique. The rate constant k_{obsd} for the ligand exchange reaction of H_2O in the transient [Cr(TPP)(Cl)(H_2O)] with pyridine was found to exhibit a bell-shaped pyridine-concentration dependence. The value of k_{obsd} initially increases with an increase in [Py]. After reaching the maximum value, k_{obsd} decreases smoothly with an increase in [Py]. These results are interpreted in terms of the formation of a dead-end complex, [Cr(TPP)(Cl)(HO−H···Py)], at the high pyridine concentration. Such a hydrogen-bonded complex was isolated as a stable product when [Cr(TPP)(Cl)(H_2O)] was recrystallized from a solvent containing 2-methylpyridine, which does not directly bind to the chromium atom due to the steric hindrance caused by the methyl group of 2-methylpyridine, and its molecular structure was investigated by X-ray crystallography. In this paper, we describe the chemical properties of this newly found complex together with the mechanism of the photochemical reaction of the chromium(III) porphyrins in solution.

Experimental Section

General Information. (Aqua)(chloro)(5,10,15,20-tetraphenylporphyrinato)chromium(III), [Cr(TPP)(Cl)(H_2O)], was prepared according to the reported procedure.[11] Pyridine and 2-methylpyridine (2-MePy) dried over solid potassium hydroxide were fractionally distilled before use. 3-Cyanopyridine was recrystallized from a mixture of *o*-xylene and hexane. Toluene was refluxed on sodium, and then distilled. Spectroscopic grade dichloromethane (Nacarai Tesque, Inc.) was used without further purification. The preparation of the polystyrene film doped with the chromium(III) porphyrins was previously described.[8] The solution of [Cr(TPP)(Cl)(Py)] in dichloromethane or toluene was prepared by adding Py to the corresponding solution of [Cr(TPP)(Cl)(H_2O)]. Dark violet crystals for the X-ray crystallography including [Cr(TPP)(Cl)(H_2O)] and 2-MePy were obtained by slow evaporation of a $CHCl_3$−toluene solution. Anal. Calcd for $C_{56}H_{44}N_6OClCr$: C, 74.37; H, 4.90; N, 9.29. Found: C, 74.07; H, 4.95; N, 8.99.

UV−vis absorption spectra were recorded on a Hitachi U-3000 spectrophotometer. The concentration of water in the toluene and dichloromethane was determined using a Karl Fischer titrator (CA-06, Mitsubishi Chemical Co., Ltd.). Laser photolysis studies were carried out with a Nd:YAG laser (Model Surelite 10, Continuum) equipped with second (532 nm) and third (355 nm) harmonic generators. The energy and duration of the laser pulse were, respectively, 100 mJ/pulse and ca. 6 ns. The detection system of the transient was previously described.[7] The concentration of the chromium(III) porphyrins was ca. 10^{-5} mol kg^{-1}. The extraneous ligand concentrations were always more than 10^{-4} mol kg^{-1}. The decay analysis of the transient species was carried out using the nonlinear least-squares method. The standard deviation for the mean value of the observed first-order rate constant k_{obsd} was less than ±3%.

X-ray Crystallography. A prismatic crystal having the approximate dimensions of 0.20 × 0.25 × 0.30 mm was mounted on a glass fiber. X-ray diffraction data were collected at −100 °C on a Rigaku RAXIS-RAPID diffractometer with graphite-monochromated Mo Kα radiation (λ = 0.710 69 Å). A total of 44 images, corresponding to 220.0° oscillation angles, were collected at two different goniometer settings. The camera radius was 127.40 mm. The exposure time was 5 min/degree. Readout was performed in the 0.100 mm pixel mode. Data were processed by the PROCESS-AUTO program package. The integration of the data yielded a total of 12 794 reflections to a maximum 2θ value of 55°, 9258 of which were independent (R_{int} = 0.035). A set of 7119 reflections ($I > 2\sigma(I)$) was used for the structure determination. A numerical absorption correction using the program NUMABS[12] was applied. The structure was solved by direct methods (SIR92[13]) and expanded using Fourier techniques (DIRDIF94[14]). All non-hydrogen atoms were anisotropically refined. Hydrogen atoms except for those on O(1) were placed in idealized positions, which were not refined. All calculations were performed using the teXsan[15] crystallographic software package from the Molecular Science Corp.

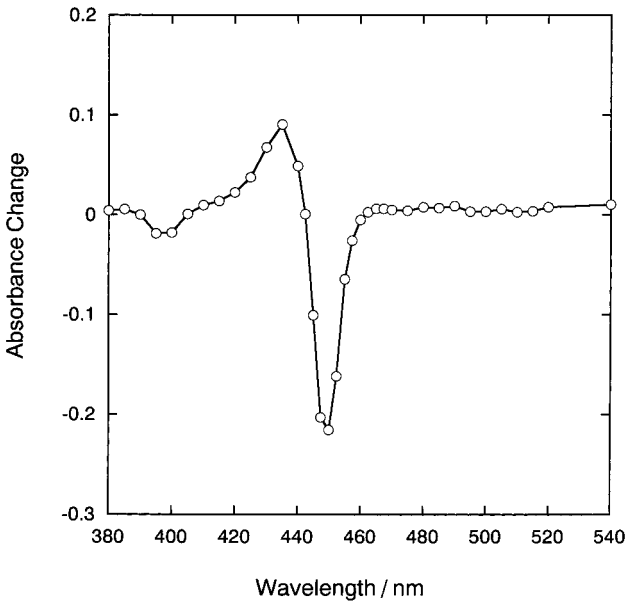

Figure 1. Transient spectrum observed for the dichloromethane solution of [Cr(TPP)(Cl)(H_2O)] in the presence of 2.02 × 10^{-3} mol kg^{-1} H_2O at 25.0 °C. The spectrum was taken at 49 ns after a 532 nm laser irradiation.

Results

Laser Photolysis of [Cr(TPP)(Cl)(H_2O)] in Dichloromethane. The photoreaction of [Cr(TPP)(Cl)(H_2O)] was studied in dichloromethane. Figure 1 shows the transient spectrum obtained at 49 ns after a 532 nm laser pulse at 25.0 °C. The spectrum exhibits a positive peak at 435 nm and a negative one at 450 nm. The transient spectrum decays according to pseudo-first-order kinetics and eventually restores the initial spectrum of [Cr(TPP)(Cl)(H_2O)]. Figure 2 shows the plot of the pseudo-first-order rate constant k_{obsd} versus the concentration of water present in the dichloromethane solution. The plot is a straight line. These findings indicate that the transient is ascribed to the five-coordinate species [Cr(TPP)(Cl)] produced by photodissociation of the axial H_2O and that the reaction observed after the laser pulse is the rebinding of the H_2O molecule to the five-coordinate [Cr(TPP)(Cl)]. Thus, k_{obsd} is given by eq 1.

$$k_{obsd} = k_{H_2O}[H_2O] + k_{-H_2O} \quad (1)$$

The slope and the intercept of the line in Figure 2 afford the bimolecular rate constant k_{H_2O} for the H_2O association of [Cr-

(11) Summerville, D. A.; Jones, R. D.; Hoffman, B. M.; Basolo, F. *J. Am. Chem. Soc*. **1977**, *99*, 8195.

(12) Higashi T. Program for Absorption Correction, Rigaku Corp., Tokyo, Japan, 1999.

(13) Altomare, A.; Burla, M. C.; Camalli, M.; Cascarano, M.; Giacovazzo, C.; Guagliardi, A.; Polidori, G. *J. Appl. Crystallogr*. **1994**, *27*, 435.

(14) Beurskens, P. T.; Admiraal, G.; Beurskens, G.; Bosman, W. P.; de Gelder, R.; Israel, R.; Smits, J. M. M. The DIRDIF-94 program system, Technical Report of the Crystallography Laboratory, University of Nijmegen, The Netherlands, 1994.

(15) Crystal Structure Analysis Package, Molecular Structure Corp., 1985, 1999.

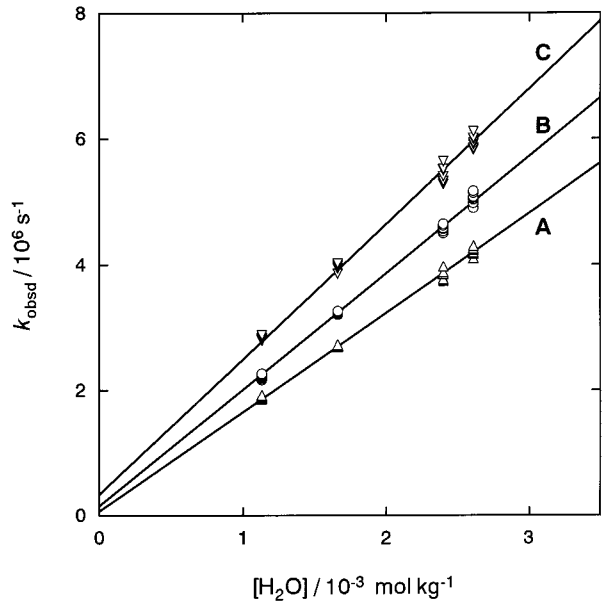

Figure 2. Dependence of the pseudo-first-order rate constant k_{obsd} of the decay of the transient spectrum for [Cr(TPP)(Cl)(H_2O)] on the concentration of H_2O in dichloromethane: $T = 15.0$ °C (A), 25.0 °C (B), and 35.0 °C (C).

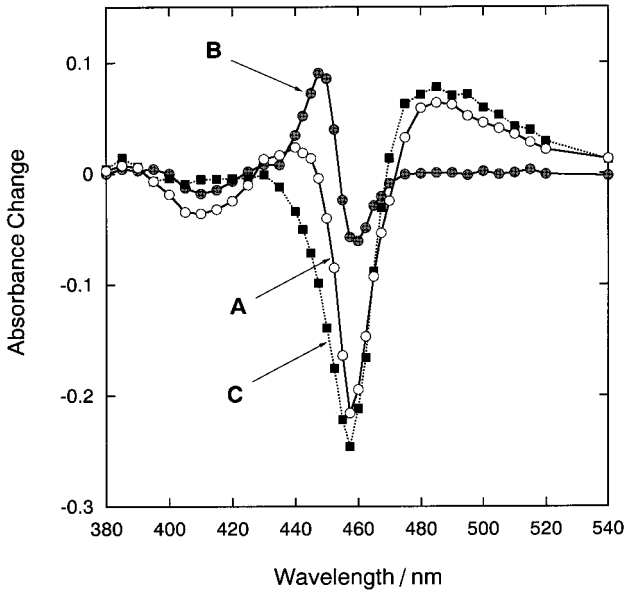

Figure 3. Transient spectra observed for the dichloromethane solution of [Cr(TPP)(Cl)(Py)] in the presence of 7.99×10^{-3} mol kg^{-1} pyridine and 1.84×10^{-2} mol kg^{-1} H_2O at 25.0 °C. The spectra were taken at 34 ns (A) and 1.2 μs (B) after a 532 nm laser irradiation. The transient spectrum observed for the polystyrene film doped with [Cr(TPP)(Cl)(Py)] taken at 59 ns is also shown (C).

(TPP)(Cl)] and k_{-H_2O} for the thermal dissociation reaction of H_2O from [Cr(TPP)(Cl)(H_2O)], respectively. The values of k_{H_2O} thus obtained are $(1.59 \pm 0.03) \times 10^9$ mol^{-1} kg s^{-1} at 15.0 °C, $(1.85 \pm 0.04) \times 10^9$ mol^{-1} kg s^{-1} at 25.0 °C, and $(2.16 \pm 0.06) \times 10^9$ mol^{-1} kg s^{-1} at 35.0 °C. The k_{-H2O} values were determined with better accuracy in the laser photolysis experiments of [Cr(TPP)(Cl)(Py)] as will be described later.

Laser Photolysis of [Cr(TPP)(Cl)(Py)]. Figure 3 shows the transient spectra observed for [Cr(TPP)(Cl)(Py)] in dichloromethane (A and B) and in polystyrene film (C) after a 532 nm laser pulsing. In a polystyrene film, the transient having a strong negative absorption around 450−460 nm and a positive one around 490 nm is ascribed to the $^6T_1$ excited state of [Cr(TPP)(Cl)(Py)], which is in thermal equilibrium with the $^4T_1$ state.[8] The excited state uniformly decays according to first-order kinetics with a rate constant of 6.2×10^6 s^{-1} at 25.0 °C. The photochemical dissociation of Py does not occur in the polystyrene film. In contrast to the case of a polystyrene film, the decay of the transient in dichloromethane containing water is biphasic; the fast step of the decay is completed within 10^{-6} s after the pulse, followed by a much slower step. The transient spectrum in dichloromethane detected at 34 ns after a laser pulse is slightly different from that in the polystyrene film. The previous studies clearly indicated that the 34-ns spectrum is composed of those of the $^6T_1$ state and the five-coordinate species [Cr(TPP)(Cl)] which is produced by the photodissociation of Py from [Cr(TPP)(Cl)(Py)].[10] The transient spectrum (Figure 3B) measured at 1.2 μs after the pulse is in good agreement with the difference spectrum between [Cr(TPP)(Cl)(H_2O)] and [Cr(TPP)(Cl)(Py)] in dichloromethane, indicating that the slower decay component is ascribed to the reaction of [Cr(TPP)(Cl)(H_2O)], which is formed by the reaction between the transient [Cr(TPP)(Cl)] and H_2O in dichloromethane.[16] The intermediate [Cr(TPP)(Cl)(H_2O)] eventually returns to [Cr(TPP)(Cl)(Py)] by the axial ligand substitution reaction with exogenous pyridine.

In a recent paper, we reported the quenching of the photodissociation of L from [Cr(TPP)(Cl)(L)] by oxygen in the toluene solution.[10] The photochemical dissociation of the axial ligand L was demonstrated to take place from both the $^4S_1$ and $^6T_1$ excited states. The quantum yields for the photodissociation of Py from [Cr(TPP)(Cl)(Py)] were determined to be 0.18 and 0.47 in the $^4S_1$ and $^6T_1$ excited states, respectively.[10] The photochemical reaction of [Cr(TPP)(Cl)(Py)] can be represented by eqs 2−10. The lifetime of the $^4S_1$ state is predicted to be

$$[Cr(TPP)(Cl)(Py)] \xrightarrow{h\nu} {}^4[Cr(TPP)(Cl)(Py)]^* \ (^4S_1) \quad (2)$$

$$^4S_1 \rightarrow {}^6[Cr(TPP)(Cl)(Py)]^* \ (^6T_1) \quad (3)$$

$$^4S_1 \rightarrow [Cr(TPP)(Cl)] + Py \quad (4)$$

$$^4S_1 \rightarrow [Cr(TPP)(Cl)(Py)] \quad (5)$$

$$^6T_1 \rightarrow [Cr(TPP)(Cl)] + Py \quad (6)$$

$$^6T_1 \rightarrow [Cr(TPP)(Cl)(Py)] \quad (7)$$

$$[Cr(TPP)(Cl)] + Py \rightleftharpoons [Cr(TPP)(Cl)(Py)] \quad (8)$$

$$[Cr(TPP)(Cl)] + H_2O \rightleftharpoons [Cr(TPP)(Cl)(H_2O)] \quad (9)$$

$$[Cr(TPP)(Cl)(H_2O)] + Py \rightarrow [Cr(TPP)(Cl)(Py)] + H_2O \quad (10)$$

shorter than the laser pulse duration (6 ns). Thus, the transients detected at 34 ns after the pulse are the $^6T_1$ state of [Cr(TPP)(Cl)(Py)] and [Cr(TPP)(Cl)]. The rate constants for the decay of the $^6T_1$ state at 25.0 °C are obtained as 9.1×10^6 and 1.1×10^7 s^{-1} in degassed dichloromethane and toluene, respectively, by analyzing the reaction curve monitored around 490 nm. These values are larger than that (6.2×10^6 s^{-1}) measured in the polystyrene film.[8]

Axial Substitution Reaction. As mentioned above, the laser photolysis of [Cr(TPP)(Cl)(Py)] in dichloromethane and toluene containing water produces [Cr(TPP)(Cl)(H_2O)] as an intermedi-

(16) Existence of a water-bound complex, [Cr(TPP)(Cl)(H_2O)], was evidenced by the X-ray crystallography[7] and laser photolysis of [Cr(TPP)(Cl)(H_2O)] described in this paper.

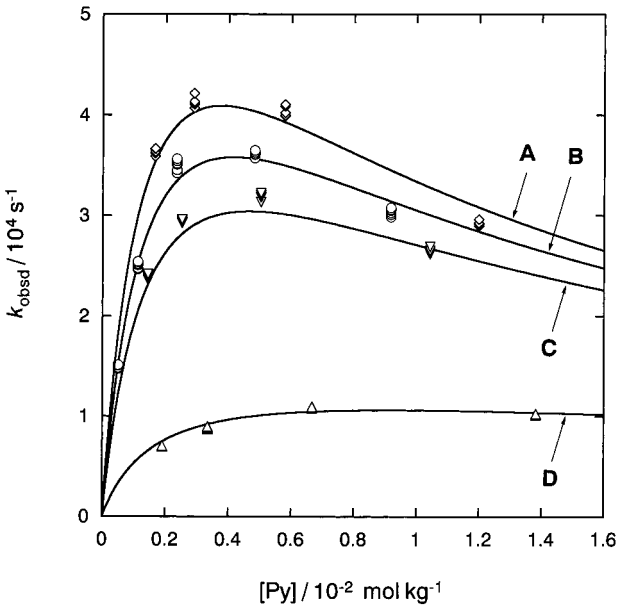

Figure 4. Pseudo-first-order rate constant k_{obsd} of the decay of [Cr(TPP)(Cl)(H_2O)] as a function of the concentration of pyridine for the laser photolysis of [Cr(TPP)(Cl)(Py)] in toluene: C_{H_2O}/mol $kg^{-1} = 3.8 \times 10^{-3}$ (A), 4.5×10^{-3} (B), 5.8×10^{-3} (C), and 2.2×10^{-2} (D). $T = 25.0$ °C.

ate. The rates for the axial substitution reaction of the bound H_2O in [Cr(TPP)(Cl)(H_2O)] by Py (eq 10) were measured under the pseudo-first-order conditions where H_2O and Py were present in a large excess over the porphyrin complex. The decay of [Cr(TPP)(Cl)(H_2O)] strictly followed the pseudo-first-order kinetics. The rate constants k_{obsd} for the substitution reaction were determined from the change of the absorbance in the Soret band region. Figure 4 shows the plot of k_{obsd} vs [Py] measured at various concentrations of H_2O in the toluene solution. At a given [H_2O], the plot of k_{obsd} exhibits a bell-shaped [Py] dependence; i.e., k_{obsd} initially increases with an increase in [Py], but it begins to decrease at a higher [Py]. The transient spectrum of [Cr(TPP)(Cl)(H_2O)] is almost invariant to the pyridine concentrations studied.

The substitution reaction of H_2O in [Cr(TPP)(Cl)(H_2O)] with the ligand L has been interpreted in terms of a dissociative mechanism.[7]

$$[Cr(TPP)(Cl)(H_2O)] \underset{k_{H_2O}}{\overset{k_{-H_2O}}{\rightleftharpoons}} [Cr(TPP)(Cl)] + H_2O \quad (11)$$

$$[Cr(TPP)(Cl)] + L \xrightarrow{k_L} [Cr(TPP)(Cl)(L)] \quad (12)$$

Here, [Cr(TPP)(Cl)] represents the reactive five-coordinate intermediate. By applying the steady-state approximation to the intermediate, the rate constant k_{obsd} is simply expressed as

$$k_{obsd} = k_{-H_2O}k_L[L](k_{H_2O}[H_2O] + k_L[L])^{-1} \quad (13)$$

Equation 13 predicts that, at a given H_2O concentration, k_{obsd} asymptotically increases with an increase in [L]. The experimental values of k_{obsd} obtained for L = 3-CNPy were explained by eq 13 when [3-CNPy] $< 1 \times 10^{-2}$ mol kg^{-1}.[7] The rate constant k_{obsd}, obtained for L = Py at low Py concentration is also well expressed by eq 13.

In the present study, we measured the values of k_{obsd} for L = Py at much higher concentrations, and found that k_{obsd} exhibits a bell-shaped [Py] dependence as shown in Figure 4. This

Chart 1

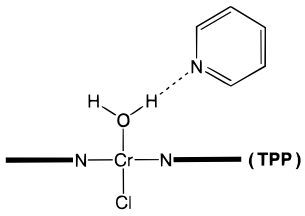

I

implies that the rate for the substitution reaction of H_2O in [Cr(TPP)(Cl)(H_2O)] with Py slows at higher concentrations of Py. Here, we consider that at the higher concentrations of Py, an axial H_2O in [Cr(TPP)(Cl)(H_2O)] interacts with exogenous pyridine to yield the hydrogen-bonded species **I**, [Cr(TPP)(Cl)(HOH- - -Py)] (Chart 1), as a dead-end complex:

$$[Cr(TPP)(Cl)(H_2O)] + Py \overset{K_L}{\rightleftharpoons} [Cr(TPP)(Cl)(HOH- - -Py)] \quad (14)$$

On the basis of the assumptions that (i) the dead-end complex is inert against the direct substitution reaction of (HOH- - -Py) with Py, (ii) the intramolecular ligand substitution reaction (eq 15) does not occur, and (iii) the pyridine-substitution reaction

$$[Cr(TPP)(Cl)(HOH- - -Py)] \rightarrow [Cr(TPP)(Cl)(Py)] + H_2O \quad (15)$$

takes place according to the combination of eqs 11, 12, and 14, the rate constant k_{obsd} is formulated as

$$k_{obsd} = k_{-H_2O}k_L[Py](k_{H_2O}[H_2O] + k_L[Py])^{-1}(1 + K_L[Py])^{-1} \quad (16)$$

Equation 16 explains the experimental values of k_{obsd} represented as functions of [H_2O] and [Py] well. The rate constants k_{-H_2O}, the ratio k_{H_2O}/k_L, and the equilibrium constant K_L were determined by the curve fitting of k_{obsd} using eq 16 and a least-squares fitting program. We found that, without using assumptions i and ii, the curve fitting of k_{obsd} does not go well. Figure S1 in the Supporting Information shows the plots of k_{obsd} vs [3-CNPy] at a constant H_2O concentration for the reaction of [Cr(TPP)(Cl)(H_2O)] with 3-CNPy obtained in the laser photolysis of [Cr(TPP)(Cl)(3-CNPy)]. A similar bell-shaped ligand-concentration dependence of k_{obsd} was clearly observed. The values of k_{-H_2O}, k_{H_2O}/k_L, and K_L were determined in the temperature range 15.0−35.0 °C. From the van't Hoff and Eyring plots, the kinetic and thermodynamic parameters for each process were evaluated. In Table 1 are listed $\Delta H_{-H_2O}^{\ddagger}$ and $\Delta S_{-H_2O}^{\ddagger}$ for k_{-H_2O}, $\Delta H_{H_2O}^{\ddagger} - \Delta H_L^{\ddagger}$ and $\Delta S_{H_2O}^{\ddagger} - \Delta S_L^{\ddagger}$ for k_{H_2O}/k_L, and ΔH_L^0 and ΔS_L^0 for K_L obtained with L = Py and 3-CNPy in toluene. The laser photolysis studies of the pyridine complex [Cr(TPP)(Cl)(Py)] in dichloromethane were also carried out. The plots of k_{obsd} vs [Py] are shown in Figures S2 and S3. Obtained kinetic and thermodynamic parameters are listed in Table 1.

As mentioned above, the rate constant k_{H_2O} was directly determined in the laser photolysis studies of [Cr(TPP)(Cl)(H_2O)] in dichloromethane. The corresponding rate constant for the reaction in the toluene solution had been previously obtained.[7] With the use of k_{H_2O} and the k_{H_2O}/k_L ratio, the rate constant k_L for the association of L to [Cr(TPP)(Cl)] can be determined. Table 2 lists the rate constants and the kinetic parameters thus obtained. The second-order rate constants of these reactions are

Table 1. Kinetic and Thermodynamic Parameters[a] for the Water Substitution Reaction of [Cr(TPP)(Cl)(H_2O)] by the Pyridine Base L[b]

	solvent	
	toluene	dichloromethane
k_{-H_2O}/s^{-1}	3.86×10^5	1.57×10^5
k_{H_2O}/k_L (L = Py)	2.07	1.29
K_L/mol^{-1} kg (L = Py)	5.48×10^2	1.25×10^3
k_{H_2O}/k_L (L = 3−CNPy)	1.97	
K_L/mol^{-1} kg (L = 3−CNPy)	6.89×10	
$\Delta H_{-H_2O}^{\ddagger}$	51.3 ± 1.7	56.3 ± 1.4
$\Delta S_{-H_2O}^{\ddagger}$	34.2 ± 5.5	43.3 ± 4.5
$\Delta H_{H_2O}^{\ddagger} - \Delta H_L^{\ddagger}$ (L = Py)	-6.9 ± 1.4	1.6 ± 0.6
$\Delta S_{H_2O}^{\ddagger} - \Delta S_L^{\ddagger}$ (L = Py)	-17.0 ± 4.7	7.4 ± 1.9
ΔH_L° (L = Py)	-40.7 ± 1.2	-46.4 ± 1.4
ΔS_L° (L = Py)	-83.9 ± 4.0	-96.3 ± 4.7
$\Delta H_{H_2O}^{\ddagger} - \Delta H_L^{\ddagger}$ (L = 3-CNPy)	-10.8 ± 2.0	
$\Delta S_{H_2O}^{\ddagger} - \Delta S_L^{\ddagger}$ (L = 3-CNPy)	-30.7 ± 6.9	
ΔH_L° (L = 3-CNPy)	-37.8 ± 2.3	
ΔS_L° (L = 3-CNPy)	-91.6 ± 7.8	

[a] ΔH/kJ mol^{-1}, ΔS/J mol^{-1} K^{-1}. [b] Values of rate and equilibrium constants were calculated by using the determined $\Delta H^{\ddagger}$, $\Delta S^{\ddagger}$, ΔH°, and ΔS°.

Table 2. Kinetic Parameters for the Reaction of the Five-Coordinate Complex [Cr(TPP)(Cl)] with the Entering Ligand L

solvent	L	k_L/mol^{-1} kg s^{-1} (25.0 °C)	$\Delta H_L^{\ddagger}$/kJ mol^{-1}	$\Delta S_L^{\ddagger}$/J mol^{-1} K^{-1}
dichloromethane	H_2O	1.85×10^9	8.9 ± 0.4	-37.6 ± 1.4
	Py	1.43×10^9	7.3 ± 0.7	-45.0 ± 2.4
toluene	H_2O[a]	1.17×10^9	8.6 ± 0.4	-42.4 ± 1.4
	Py	5.65×10^8	15.5 ± 1.5	-25.4 ± 4.9
	3-CNPy	5.94×10^8	19.4 ± 2.0	-11.7 ± 7.0

[a] Reference 7.

very large but are, however, a little smaller than that for the diffusion-controlled reaction, the value of which is estimated to be on the order of 10^{10} mol^{-1} kg s^{-1} in these solvents. A small energy barrier implying a small activation enthalpy and a negative activation entropy indicates that the energetic cost required for orienting the reacting partners in a favorable configuration for bond formation would not be very large like other metalloporphyrins with very large rate constants (in the range of 10^8-10^9 mol^{-1} kg s^{-1}) for the axial ligand rebinding for iron(II)[17−19] and cobalt(III)[20,21] studied by the laser photolysis method.

Reaction of [Cr(TPP)(Cl)(H_2O)] and 2-Methylpyridine in Toluene. To obtain supporting evidence for the hydrogen-bonded species **I**, we examined the reaction of [Cr(TPP)(Cl)-(H_2O)] with a sterically hindered pyridine molecule. The absorption spectrum of [Cr(TPP)(Cl)(H_2O)] in toluene displays a slight change with the addition of 1×10^{-2} mol kg^{-1} 2-MePy. The absorption peak of the Soret band shifts to red only by ca. 3 nm, suggesting that the H_2O in [Cr(TPP)(Cl)(H_2O)] hardly undergoes the axial ligand exchange with the exogenous 2-MePy. Presumably, the steric effect of the methyl group in 2-MePy prohibits the axial ligation to the central chromium of the complex.

(17) Maillard, P.; Schaeffer, C.; Tétreau, C.; Lavalette, D.; Lhoste, J.-M.; Momenteau, M. *J. Chem. Soc., Perkin Trans. 2* **1989**, 1437.
(18) Dixon, D. W.; Kirmaier, C.; Holten, D. *J. Am. Chem. Soc.* **1985**, *107*, 808.
(19) Lavalette, D.; Tetreau, C.; Momenteau, M. *J. Am. Chem. Soc.* **1979**, *101*, 5395.
(20) Tait, C. D.; Holten, D.; Gouterman, M. *J. Am. Chem. Soc.* **1984**, *106*, 6, 6653.
(21) Hoshino, M.; Kogure, M.; Asano, K.; Hinohara, T. *J. Phys. Chem.* **1989**, *93*, 6655.

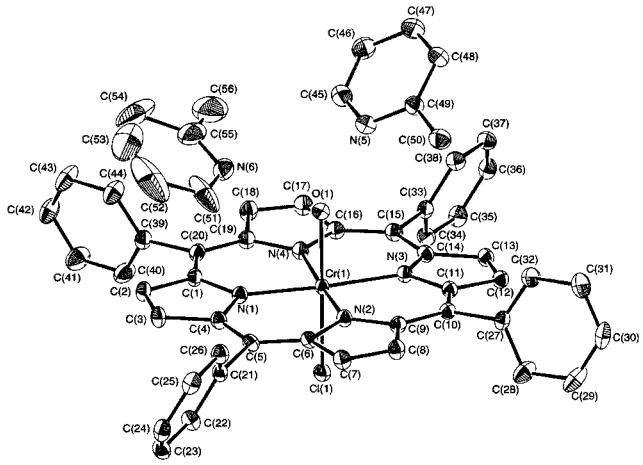

Figure 5. ORTEP diagram of the structure of the 2-MePy adduct of [Cr(TPP)(Cl)(H_2O)]. The thermal ellipsoids are drawn at the 30% probability level.

Table 3. Crystallographic Data and Experimental Details

compd	[Cr(TPP)(Cl)(H_2O)](2-MePy)$_2$	Z	2
		V, Å^3	2272.4(3)
empirical formula	$C_{56}H_{44}N_6ClCrO$	μ(Mo Kα), cm^{-1}	3.59
		transm factor	0.9057−0.9389
M	904.45	cryst size, mm^3	$0.20 \times 0.25 \times 0.30$
cryst system	triclinic	d_{calcd}, g cm^{-3}	1.322
space group	P-1	λ(Mo Kα), Å	0.710 69
a, Å	11.7727(5)	T, °C	−100
b, Å	19.277(2)	$2\theta_{max}$, deg	55
c, Å	10.3870(3)	R^a	0.058
α, deg	90.104(8)	$R_w{}^b$	0.089
β, deg	105.424(5)		
γ, deg	89.935(7)		

[a] $R = \sum||F_o| - |F_c||/\sum|F_o|$. [b] $R_w = (\sum w(|F_o| - |F_c|)^2/\sum w|F_o|^2)^{1/2}$, $w = [\sigma_c^2(F_o)+(p^2/4)|F_o|^2]^{-1}$, $p = 0.0700$.

Table 4. Selected Bond Lengths (Å) and Angles (deg) for the Porphyrin Complex

Cr(1)−Cl(1)	2.3114(7)	Cr(1)−N(3)	2.057(2)
Cr(1)−O(1)	2.057(2)	Cr(1)−N(4)	2.035(2)
Cr(1)−N(1)	2.046(2)	O(1)−N(5)	2.750(3)
Cr(1)−N(2)	2.035(2)	O(1)−N(6)	2.781(3)
Cl(1)−Cr(1)−O(1)	178.75(6)	N(1)−Cr(1)−N(2)	89.90(8)
Cl(1)−Cr(1)−N(1)	90.94(6)	N(1)−Cr(1)−N(3)	176.60(8)
Cl(1)−Cr(1)−N(2)	91.23(6)	N(1)−Cr(1)−N(4)	90.43(8)
Cl(1)−Cr(1)−N(3)	92.46(6)	N(2)−Cr(1)−N(3)	90.14(8)
Cl(1)−Cr(1)−N(4)	92.27(7)	N(2)−Cr(1)−N(4)	176.48(9)
O(1)−Cr(1)−N(1)	88.00(8)	N(3)−Cr(1)−N(4)	89.33(8)
O(1)−Cr(1)−N(2)	88.11(8)	Cr(1)−O(1)−N(5)	118.3(1)
O(1)−Cr(1)−N(3)	88.60(8)	Cr(1)−O(1)−N(6)	121.2(1)
O(1)−Cr(1)−N(4)	88.40(8)		

The molecular structure of the complex including [Cr(TPP)-(Cl)(H_2O)] and 2-MePy is shown in Figure 5. The crystallographic data are listed in Table 3. The angles α and γ are close to 90°, so the crystal system was checked for a monoclinic lattice. A 2-fold axis parallel to the b axis was found to be absent because the agreement factor between the h,k,l and $-h,k,-l$ reflections was too large. On the basis of a statistical analysis of the intensity distribution, and the successful solution and refinement of the structure, the space group was determined to be P-1. Selected bond lengths and bond angles are given in Table 4, and complete listings of the structural data are given in the Supporting Information.

As shown in Figure 5, 1 mol of [Cr(TPP)(Cl)(H_2O)] accompanies 2 mol of 2-MePy via a hydrogen bond. The N(5)−O(1) and N(6)−O(1) distances are 2.750(3) and 2.781(3) Å, respectively. The angles of Cr(1)−O(1)−N(5) and Cr(1)−O(1)−

N(6) are 118.3(1)° and 121.2(1)°, respectively. One of the two 2-MePy molecules is approximately positioned over the *meso*-C atom of the porphyrin, and the other is over the pyrrole ring, with the angle N(5)−O(1)−N(6) being 104.0(1)° as shown in Figure S5. The latter 2-MePy molecule is so heavily disordered that the exact distances and angles among the N(6) and C(51)−C(56) atoms were not obtained. Although the crystal structure was considered, it was not clear why one of the 2-MePy molecules is significantly disordered in the crystal.

These hydrogen bonds affect the structure of the [Cr(TPP)(Cl)(H_2O)] unit, especially for the axial bond lengths. The axial Cr−O bond shortens from 2.239(3) to 2.057(2) Å, and the axial Cr−Cl bond is elongated from 2.242(3) to 2.3114(7) Å due to the hydrogen bond formation between the axial water molecule and 2-MePy as compared with the structure of [Cr(TPP)(Cl)(H_2O)].[7] The Cr−Cl bond length of the present complex is close to that for [Cr(TPP)(Cl)(Py)] (2.311(2) Å)[7] and [Cr(TPP)(Cl)(1-MeIm)] (2.317(2) Å, 1-MeIm = 1-methylimidazole).[22] On the other hand, the hydrogen bond has little effect on the other structural features. The average Cr−N_p bond length of 2.043 Å is almost the same as those of the other chromium(III) porphyrins. The Cl−Cr−O angle of 178.75(6)° and the N_p−Cr−O angles, which span the range 88.00(8)−88.60(8)°, are consistent with a modest off-plane displacement of the central chromium atom toward the Cl atom. A formal diagram of the porphyrin core is shown in Figure S4, in which the perpendicular displacement of each atom from the 24-atom porphyrin mean plane is displayed. The porphyrin core is approximately planar, and the individual atomic displacements are all <0.14 Å. The *meso*-phenyl groups are moderately tilted from the porphyrin normal. Individual dihedral angles between the 24-atom porphyrin mean plane and the phenyl rings range from 66.15(8)° to 79.89(10)°.

On the basis of these structural features of the complex, the small shift in the absorption bands of [Cr(TPP)(Cl)(H_2O)] in toluene observed with the addition of 2-MePy is interpreted in terms of the formation of the hydrogen bond between the N atom in 2-MePy and the H_2O ligand of [Cr(TPP)(Cl)(H_2O)]. It is likely that the formation of the hydrogen bond does not cause a remarkable difference in the absorption spectra between [Cr(TPP)(Cl)(H_2O)] and its 2-MePy adduct.

The laser photolysis studies of [Cr(TPP)(Cl)(H_2O)] in solution containing 1.0×10^{-2} mol kg^{-1} 2-MePy were carried out to elucidate the effects of the hydrogen bond on the photodissociation of the axial ligands. The detected transients are mostly attributed to the $^6T_1$ excited state. The photodissociation of the axial ligand is markedly suppressed due to the formation of the hydrogen bond between the axial water and 2-MePy. The hydrogen bond formation increases the Cr−O bond strength, which is reflected in the shortening of the Cr−O bond length, resulting in the decrease of the yield for photodissociation of the axial ligand.

Discussion

Reagent grade toluene and dichloromethane contain at least 1.0×10^{-3} mol kg^{-1} water. Recrystallization of the chromium(III)−TPP complex from these solutions gives [Cr(TPP)(Cl)(H_2O)], in which a water molecule is coordinated to the axial position.[16] Such axial coordination of water has also been observed for iron(II) porphyrins in toluene.[17] The equilibrium constant for the H_2O binding to the iron(II) porphyrins is on the order of 10^3−10^4 mol^{-1} kg. These values are comparable to that obtained with [Cr(TPP)(Cl)] in the present study, i.e., 1.2×10^4 mol^{-1} kg in dichloromethane and 3.0×10^3 mol^{-1} kg in toluene at 25.0 °C.

The axial water in [Cr(TPP)(Cl)(H_2O)] readily undergoes a ligand exchange reaction in the presence of nitrogenous bases to yield [Cr(TPP)(Cl)(L)] (L = Py, 1-methylimidazole, 1,2-dimethylimidazole). The molecular structures of these complexes have been investigated by X-ray crystallography.[7,22] The present work has shown that 2-methylpyridine forms a hydrogen bond with the axial H_2O in [Cr(TPP)(Cl)(H_2O)] to yield a stable product in the crystal and that pyridine also forms a hydrogen bond with [Cr(TPP)(Cl)(H_2O)] in solution. However, the hydrogen-bonded species [Cr(TPP)(Cl)(HO−H···Py)] is not stable and reverts to [Cr(TPP)(Cl)(Py)]. It is noteworthy that the hydrogen bond formation between the axial water of the metalloporphyrin and a nitrogenous base has been observed for metmyoglobin.[23] The axial water coordinated to the central iron(III) atom in metmyoglobin forms a hydrogen bond with the distal histidine. Probably, the hydrogen bond formation increases the basicity of the oxygen atom of the axial H_2O, leading to the stable Fe(III)−O bond in metmyoglobin.

The first-row transition-metal complexes of the porphyrins have the excited electronic states $^{1,3}(\pi,d)^*$, $^{1,3}(d,\pi)^*$, and $^{1,3}(d,d)^*$, which lie below the porphyrin-localized S_1 excited state in energy.[24] A number of studies on the photoelimination of axial ligands from iron(II), cobalt(II), and cobalt(III) porphyrins have shown that the dissociation of the ligand occurs from the excited states involving an antibonding d_z^2 orbital of the central metal.[3] In contrast to the iron(II), cobalt(II), and cobalt(III) porphyrins, the photodissociation of the axial ligand from chromium(III) porphyrins has been demonstrated to occur in both the $^4S_1$ and $^6T_1$ states.[10] The dissociation yield of the axial ligand in both the $^4S_1$ and $^6T_1$ states increases with a decrease in the bond strengths between the central Cr atom and the axial ligand L.[10]

The laser photolysis studies of [Cr(TPP)(Cl)(Py)] in toluene and dichloromethane containing water and pyridine have shown that the initially produced [Cr(TPP)(Cl)] reacts with H_2O to yield [Cr(TPP)(Cl)(H_2O)]. The axial H_2O in [Cr(TPP)(Cl)(H_2O)] is then replaced by the exogenous Py, thus returning to [Cr(TPP)(Cl)(Py)]. Kinetic studies revealed that, at higher concentrations of pyridine, [Cr(TPP)(Cl)(H_2O)] interacts with Py to give the hydrogen-bonded species **I** as illustrated in Chart 1. As mentioned above, the absorption spectrum of the 2-MePy adduct of [Cr(TPP)(Cl)(H_2O)] is found to be very similar to that of [Cr(TPP)(Cl)(H_2O)] in the Soret band region. The interaction between pyridine and the axial H_2O in **I** is, therefore, postulated to be too weak to cause the spectral change.

The rate for the ligand exchange reaction of **I** by Py is very slow in comparison with that of [Cr(TPP)(Cl)(H_2O)]. This implies that the hydrogen bonding may increase the basicity of the oxygen atom of the axial H_2O, resulting in an increase in the strength of the Cr−O bond. The kinetic studies for the exchange reaction of the axial HO−H···Py in **I** by exogenous pyridine have shown that the sequential dissociation of Py and then H_2O from **I** gives a coordinately unsaturated [Cr(TPP)(Cl)]. Then, [Cr(TPP)(Cl)] reacts with exogenous Py, leading to the formation of [Cr(TPP)(Cl)(Py)].

The formation of the hydrogen-bonded species **II**, [Cr(TPP)(Cl)(HO−H···3-CNPy)], is also observed when 3-CNPy is used as an exogenous ligand. The equilibrium constant, K_L, for the

(22) Inamo, M.; Nakajima, K. *Bull. Chem. Soc. Jpn.* **1998**, *71*, 883.

(23) Antonini, E.; Brunori, M. *Hemoglobin and Myoglobin in Their Reactions with Ligands*; North-Holland: Amsterdam, 1971.

(24) Dolphine, D., Ed. *The Porphyrins*; Academic Press: New York, 1979.

formation of **II** determined from the kinetic analysis is smaller than that of **I** by a factor of ca. 8. This result is interpreted in terms of the difference in the basicity between Py and 3-CNPy. These complexes, **I** and **II**, are not equilibrium species, and eventually return to [Cr(TPP)(Cl)(Py)] and [Cr(TPP)(Cl)-(3-CNPy)], respectively.

It has been recognized that the porphyrin ligand enhances the water exchange rate of metal ions, and this effect has been clearly demonstrated for the iron(III) complexes. Kinetic parameters for the axial water exchange of the Fe(III)−TMPyP complex (TMPyP = 5,10,15,20-tetrakis(4-*N*-methylpyridyl)-porphyrin) and the Fe(III)−TPPS complex (TPPS = 5,10,15,-20-tetrakis(4-sulfonatophenyl)porphyrin) have been determined to be $k = 7.8 \times 10^5\ s^{-1}$ (25 °C), $\Delta H^{\ddagger} = 58$ kJ mol^{-1}, and $\Delta S^{\ddagger} = 61$ J mol^{-1} K^{-1} for the former, and $k = 1.4 \times 10^7\ s^{-1}$ (25 °C), $\Delta H^{\ddagger} = 57$ kJ mol^{-1}, and $\Delta S^{\ddagger} = 84$ J mol^{-1} K^{-1} for the latter.[25] The water exchange rate is enhanced by a factor of 10^4−10^5 over that of the hydrated Fe(III) ion: $k = 1.6 \times 10^2\ s^{-1}$ (25 °C), $\Delta H^{\ddagger} = 64$ kJ mol^{-1}, and $\Delta S^{\ddagger} = 12$ J mol^{-1} K^{-1}.[26] Similar acceleration effects of the porphyrin ligand on the exchange rate are observed in the present work; the dissociation rate of H_2O from [Cr(TPP)(Cl)(H_2O)] in toluene is found to be $3.86 \times 10^5\ s^{-1}$ (25 °C). This value is much greater than that ($2.4 \times 10^{-6}\ s^{-1}$ at 25 °C) from the hydrated Cr(III) ions in water.[27] The kinetic parameters for the axial H_2O exchange are $\Delta H^{\ddagger} = 51.3$ kJ mol^{-1} and $\Delta S^{\ddagger} = 34.2$ J mol^{-1} K^{-1} for [Cr(TPP)(Cl)(H_2O)] in toluene, and $\Delta H^{\ddagger} = 109$ kJ mol^{-1}, and $\Delta S^{\ddagger} = 12$ J mol^{-1} K^{-1} for the hydrated Cr(III) ions in water.[27] Although the solvent is different in the above two systems, it was concluded that [Cr(TPP)(Cl)(H_2O)] exchanges the axial H_2O more readily than the hydrated Cr(III) ions. These results are well explained by the difference in the mechanism of the H_2O exchange reaction between [Cr(TPP)(Cl)(H_2O)] and the Cr(III) ions; the former proceeds via a dissociative mechanism, and the latter via an associative mechanism. In general, the intermediates of the ligand exchange reactions are the five-coordinate species for the dissociative mechanism and the seven-coordinate species for the associative mechanism. In the case of [Cr(TPP)(Cl)(H_2O)], the intermediate is the five-coordinate species, indicating that the porphyrin ligand stabilizes the five-coordinate species [Cr(TPP)(Cl)] rather than the seven-coordinate species as an intermediate for the ligand exchange reactions.

Supporting Information Available: Figures reporting the ligand concentration dependence of k_{obsd} for the reaction systems [Cr(TPP)-(Cl)(3-CNpy)] in toluene and [Cr(TPP)(Cl)(Py)] in dichloromethane, a formal diagram of the porphyrin core, top and side views of the complex, tables reporting bond distances and angles and positional and thermal parameters for the structurally characterized porphyrin complex, and on X-ray crystallographic file in CIF format. This material is available free of charge via the Internet at http://pubs.acs.org.

IC0002059

(25) Ostrich, I. J.; Liu, G.; Dodgen, H. W.; Hunt, J. P. *Inorg. Chem.* **1980**, *19*, 619.
(26) Grant, M.; Jordan, R. B. *Inorg. Chem.* **1981**, *20*, 55.
(27) Xu, F.-C.; Krouse, H. R.; Swaddle, T. W. *Inorg. Chem.* **1985**, *24*, 267.